

Parallel Pathways in Cytochrome c_{551} Folding

Stefano Gianni¹, Carlo Travaglini-Allocatelli¹, Francesca Cutruzzolà¹
Maurizio Brunori^{1*}, M. C. Ramachandra Shastry² and Heinrich Roder²

¹Istituto Pasteur-Fondazione Cenci Bolognetti, Dipartimento di Scienze Biochimiche e Istituto di Biologia e Patologia Molecolari del CNR, Università di Roma "La Sapienza" Piazzale A. Moro 5, 00185 Rome, Italy

²Institute for Cancer Research Fox Chase Cancer Center Philadelphia, PA 19111, USA

The folding of cytochrome c_{551} from *Pseudomonas aeruginosa* was previously thought to follow a simple sequential mechanism, consistent with the lack of histidine residues, other than the native His16 heme ligand, that can give rise to mis-coordinated species. However, further kinetic analysis reveals complexities indicative of a folding mechanism involving parallel pathways. Double-jump interrupted refolding experiments at low pH indicate that ~50% of the unfolded cytochrome c_{551} population can reach the native state *via* a fast (10 ms) folding track, while the rest follows a slower folding path with populated intermediates. Stopped-flow experiments using absorbance at 695 nm to monitor refolding confirm the presence of a rapidly folding species containing the native methionine-iron bond while measurements on carboxymethylated cytochrome c_{551} (which lacks the Met-Fe coordination bond) indicate that methionine ligation occurs late during folding along the fast folding track, which appears to be dominant at physiological pH. Continuous-flow measurements of tryptophan-heme energy transfer, using a capillary mixer with a dead time of about 60 μ s, show evidence for a rapid chain collapse within 100 μ s preceding the rate-limiting folding phase on the milliseconds time scale. A third process with a time constant in the 10–50 ms time range is consistent with a minor population of molecules folding along a parallel channel, as confirmed by quantitative kinetic modeling. These findings indicate the presence of two or more slowly inter-converting ensembles of denatured states that give rise to pH-dependent partitioning among fast and slow-folding pathways.

© 2003 Elsevier Ltd. All rights reserved

Keywords: folding pathways; intermediates; kinetic partitioning; cytochrome *c*; Chevron plot

*Corresponding author

Introduction

Protein folding studies have focused over the last decades on the elucidation of the kinetic pathways for unfolding and refolding reactions. In particular, characterization of the structure and stability of partially folded states was believed to provide a key for defining the mechanism of protein folding; thus, the problem of understanding how proteins fold was addressed by identifying and characterizing transition states and

metastable structures, thought to be obligatory intermediates along the folding pathway.^{1–3} The identification of kinetic traps in the folding of several proteins and theoretical models have led to alternative views of protein folding. In particular, a more general picture in which a global bias in the energy landscape (the folding “funnel”) guides diffusion between non-native conformations and the native state has emerged.^{4–6} According to this view, there is a great number of possible folding pathways for a given protein, which are statistically selected according to their relative activation energies.

Mammalian cytochrome *c* has played a central role in protein folding studies. In the last ten years, its folding mechanism has been studied in detail by means of different techniques, including millisecond^{7–9} and, more recently, sub-millisecond transient emission and absorption spectroscopies.^{10–15} In addition to kinetic traps due

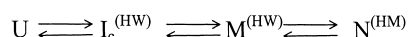
Present address: S. Gianni, Cambridge Centre for Protein Engineering, Medical Research Council, Hills Road, Cambridge CB2 2QH, UK; M. C. R. Shastry, Colgate-Palmolive Company, Piscataway, NJ 08855, USA.

Abbreviations used: Cyt, *c*, cytochrome *c*; Cm-cyt, c_{551} , carboxy-methyl cyt c_{551} ; wt, wild-type.

E-mail address of the corresponding author: maurizio.brunori@uniroma1.it

to proline *cis/trans* isomerisation or miscoordinated states, the kinetic folding mechanism emerging from these investigations involves the rapid (60–90 μ s) formation of an ensemble of relatively compact states with partially quenched Trp fluorescence,^{12,15} followed by the formation of the native state (> ms), which involves as a critical step the interactions between the N and C-terminal helices.^{7,16,17}

Kinetic approaches to elucidating the folding mechanism of cytochrome *c* (cyt *c*) took advantage of the presence of the covalently bound heme group, which serves as a useful optical marker, both because of its axial coordination changes and its efficient Trp fluorescence quenching. Altogether these studies have shown that the productive folding pathway of horse cyt *c*, starting from the unfolded polypeptide, proceeds through a compact intermediate, $I_c^{(HW)}$, in which the native His(18) ligand and a water molecule are coordinated to the heme iron, followed by formation of the native His(18)–Fe–Met(80) heme coordinated form, $N^{(HM)}$, during the final stages of folding.^{12,18–20} Moreover, unfolding experiments on different cytochromes *c* indicated that the Fe–Met(80) (numbering is for horse cyt *c*) deligation step is limited by a “native-like” transition state^{21,22} involving a high energy intermediate (M). Therefore a general scheme that describes the folding of cytochromes *c* is:



Scheme 1.

Where: U is the unfolded state, I_c is an early collapsed intermediate, M is a native-like intermediate lacking the Met–Fe coordination bond, N is the native state (with the distal coordination bond formed). The different iron coordination states are indicated in parentheses as HW: Fe³⁺ coordinated by His(18) and water; and HM: Fe³⁺ coordinated by His(18) and Met(80).

Other cytochromes *c*, such as cyt c_{551} from *P. aeruginosa*,²³ cyt c_2 from *Rhodobacter capsulatus*²¹ and *iso-2* cyt *c*,²⁴ present the same general folding features (i.e. a burst phase collapse in the refolding process and breaking of the Fe–Met bond limiting the rate of unfolding at high denaturant concentrations). For horse cyt *c* and *Rhodobacter* cyt c_2 , the non-linear dependence of the refolding rate on denaturant concentration (“roll-over”) has been interpreted to indicate mainly the population of a refolding intermediate; however, a study on the folding pathway of cyt c_{551} and its mutants²² led to the hypothesis that, in addition to the formation of transient aggregates,^{23,25} refolding occurs from the collapsed state *via* a broad energy barrier²⁶ in which the net charge of the protein limits the folding rate.

The experiments presented here aim at a more detailed analysis of the folding pathway of cyt c_{551} , extending the experiments to the previously

unresolved sub-milliseconds time range thanks to the continuous-flow capillary mixing apparatus recently developed.²⁷ Moreover, using interrupted refolding experiments carried out with a stopped-flow instrument, we addressed the issue of parallel folding pathways; more specifically we explored if all molecules achieve the native state *via* the same path or whether some of the molecules may refold *via* a faster route, as initially shown by Kiefhaber for lysozyme.²⁸ The results show that the micro-seconds folding kinetics of cyt c_{551} is biphasic, and that (under particular experimental conditions) approximately half of native cyt c_{551} is populated in a kinetic process consistent with previously described milliseconds processes,^{22,23} while the remainder, which folds much more rapidly, indicates the presence of an alternative folding track.

Results

According to Scheme 1, the folding mechanism of cytochromes *c* (under conditions that avoid miscoordinated off-pathway traps) involves the population of at least two transient intermediates. Additional insight into the mechanism would demand experiments to find out whether all molecules reach the native state *via* the same unique pathway or whether parallel pathways are active. Following Kiefhaber,²⁸ we carried out a double-jump interrupted refolding experiment in which: (i) unfolded cyt c_{551} is first mixed against a refolding buffer (first mix) and (ii) after a controlled delay time, refolding is interrupted by rapid addition of high concentrations of the same denaturant (second mix). This approach makes it possible to distinguish partially folded intermediates from native molecules since these states are characterized by different unfolding rates. In particular, the native protein being separated from the unfolded one by the highest energy barrier should unfold more slowly than any partially folded intermediate. According to Shastry & Roder,¹² in the case of horse cyt *c* the calculated unfolding rate for both I_c and M at high denaturant concentration (i.e. [GdnHCl] = 3 M) would be too fast (>10,000 s⁻¹) for stopped flow detection. Thus, the fractional population of native molecules formed during the delay time between first and second mix is represented by the relative amplitude of the slowest unfolding event.

Since the minimum delay time of our stopped-flow instrument is about 10 ms, we restricted ourselves to carry out this experiment at pH 3.0 in 0.4 M GdnHCl, where there is a pronounced micro-second burst phase but the observed k_{ref} is about 4 s⁻¹.²³ As shown in Figure 1(a), the time courses observed after different delay times can be described by single-exponential kinetics, as expected if only the unfolding of the native state is detectable in the milliseconds time range. The amplitude behavior of the single exponential unfolding reaction as a function of delay time

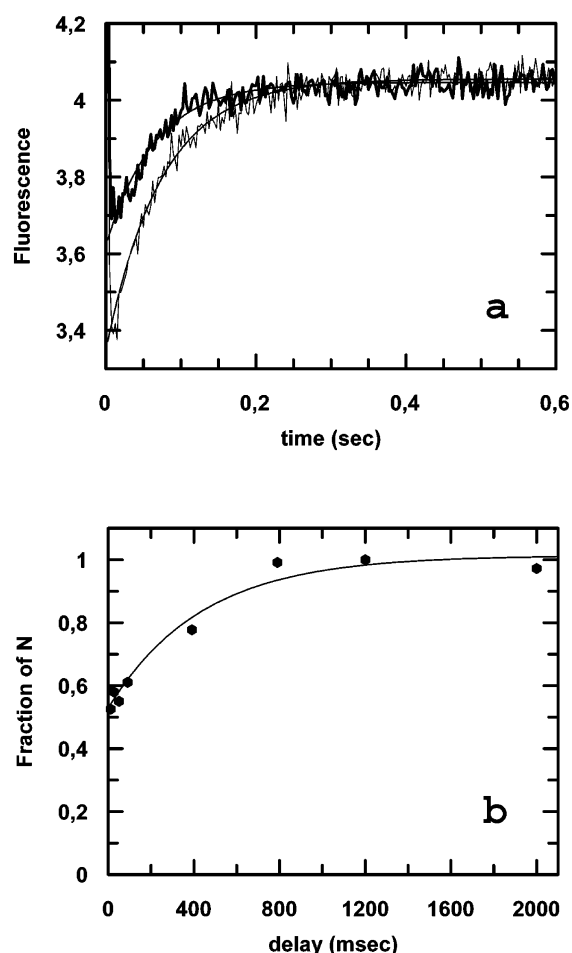


Figure 1. Double mixing interrupted-refolding on wt cyt c_{551} measured in GdnHCl at pH 3.0. (a) Representative kinetic traces for unfolding recorded after 17 ms (black trace) and four seconds (gray trace) delay time (see Results and Discussion). (b) Time course of appearance of native cyt c_{551} during refolding in 0.4 M GdnHCl at pH 3.0 and 10 °C. Continuous line corresponds to $k = 2.5 \text{ s}^{-1}$.

between the first and the second mix is depicted in Figure 1(b). Surprisingly, we found the formation of $\sim 50\%$ of the native protein even at the shortest delay time (10 ms), suggesting the presence of a fast refolding pathway that allows a fraction of the unfolded protein to reach the native state in less than 10 ms. Moreover, the rate obtained from the time dependence of the amplitude is consistent with the refolding kinetics measured from classical single mix dilution experiments under these pH and solvent conditions.²³ In the absence of kinetic partitioning events, the observed amplitude behavior as a function of delay time from the interrupted refolding experiment should extrapolate to zero at zero delay time, contrary to what is observed.

The interrupted refolding experiment clearly suggests the presence of a parallel pathway for cyt c_{551} folding. In an effort to observe the rapid folding phase directly, we carried out continuous-flow

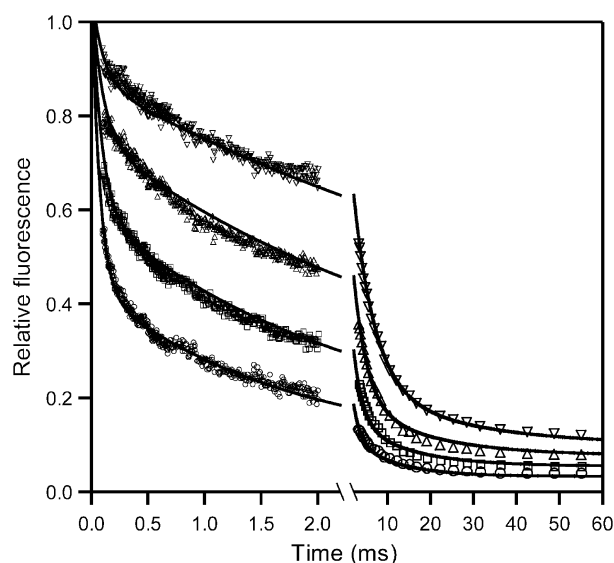


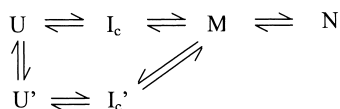
Figure 2. Tryptophan fluorescence changes during refolding of cyt c_{551} (20 μM) at different urea concentrations (0.17 M circles, 0.5 M squares, 1.0 M upper triangles, 1.5 M lower triangles in 0.1 M phosphate, pH 4.7) measured in a matching continuous-flow and stopped-flow experiments at 15 °C. The data were normalized relative to the signal of the unfolded state at 1 M urea, pH 2. The continuous lines show the time course of folding at each urea concentration predicted by Scheme 2 (see the text).

fluorescence experiments using a capillary mixer with a dead time of about 60 μs . Cyt c_{551} was fully unfolded in 1 M urea at pH 2.0, and refolding was triggered by a sixfold dilution of the denaturant with buffer at a final pH of 4.7. Representative continuous-flow refolding traces at urea concentrations from 0.17 M to 1.5 M and pH 4.7 are combined with stopped-flow traces recorded under matching conditions (Figure 2). The traces are scaled with respect to the fluorescence of the unfolded protein. The combined kinetics is well described by a sum of three exponential phases; the rate constants and amplitudes thus obtained are listed in Table 1. The amplitude of the intermediate phase increases at the expense of that of the fast phase with increasing urea concentration. At denaturant concentrations approaching the midpoint of the unfolding transition the intermediate phase becomes the dominant process, and its rate joins that of the single unfolding phase in the unfolding transition region (data not shown).

Table 1. Observable rate constants and amplitudes obtained by triple-exponential fitting of fluorescence-detected folding kinetics of cyt c_{551} at pH 4.7 and 20 °C

[Urea] (M)	λ_1 (s^{-1}) (a_1)	λ_2 (s^{-1}) (a_2)	λ_3 (s^{-1}) (a_3)
0.17	9150 (0.34)	1050 (0.22)	130 (0.17)
0.5	6900 (0.21)	790 (0.27)	160 (0.28)
1.0	2000 (0.18)	230 (0.53)	50 (0.07)
1.5	2900 (0.08)	170 (0.70)	20 (0.06)

This behavior is consistent with the transient accumulation of an on-pathway folding intermediate on the 100 μs time scale (fast phase), followed by the rate-limiting conversions of the intermediate into the native state (intermediate phase). The presence of an additional phase with minor amplitude ($\sim 5\text{--}25\%$) and a rate constant slower than the main folding phase can be explained by a minor population of molecules folding along a parallel pathway with a five to tenfold slower rate. To support this conclusion, we performed kinetic simulations using the following six-state mechanism:



Scheme 2.

Inclusion of a native-like intermediate, M , is necessary to account for the sharp bend in the $\log(k)$ versus [denaturant] plot at high denaturant concentrations,^{22,23} but has no effect on the kinetics of refolding. A possible interconversion between the I_c and I_c' states has been omitted because the direct observation of kinetic partitioning implies that the rate constants connecting I_c and I_c' are considerably slower than the fast folding reaction leading to M . The logarithm of the elementary rate constants, k_i , is assumed to vary linearly with urea concentrations.²⁹ The linear differential equations corresponding to Scheme 2 were solved numerically, resulting in predicted observable rate constants and kinetic amplitudes.²¹ Manual optimization of the elementary rate constants and kinetic m -values resulted in a set of predicted rates and amplitudes consistent with those obtained by exponential fitting of experimental kinetic traces. The family of traces as a function of urea concentration predicted by the model (continuous lines in Figure 2) provide an adequate global fit of the observed kinetics. Thus, while not all of the elementary kinetic parameters are uniquely determined by the fit, the analysis shows that Scheme 2 is consistent with the observed folding kinetics of $\text{cyt } c_{551}$ at pH 4.7. We were unable to reproduce the observed data using models with fewer states. Moreover, it is necessary to introduce a heterogeneous population of slowly interconverting denatured states, including a minor ($\sim 20\%$ under the present conditions) species, U' , which encounters a somewhat slower rate-limiting step. The minor phase on the 10–100 ms time scale is too fast to involve peptide bond isomerization as the rate-determining event and cannot be explained by heme misligation due to the absence of alternative heme ligands in $\text{cyt } c_{551}$. Our observation that about half of the population folds at a rate of 4 s^{-1} at pH 3 (Figure 1) suggests that the relative populations of U and U' vary with pH so that U' becomes the dominant species at low pH.

Qualitatively, the model also accounts for the rather complex denaturant-dependence of the observable rates and amplitudes, including the maximum in a_3 near 0.5 M urea (Table 1). Given that the relative amplitude of the slower folding track (a_3 in Table 1) drops to $\sim 10\%$ at [urea] > 0.5 M and that the corresponding folding rate at lower urea concentration is too fast for our stopped-flow apparatus (minimum delay time ~ 10 ms), we were unable to confirm the presence of parallel pathways by interrupted refolding experiments at pH values above 3.0. However, in a previous study on site-directed mutants of $\text{cyt } c_{551}$ ²² we have shown that, while pH modulates the free energies of the native state as well as intermediates and transition states, the overall folding mechanism of this small protein appears to be independent of pH. This observation allowed us to qualitatively compare double-jump interrupted refolding experiments at acidic conditions (yielding direct evidence for parallel folding pathways) with experiments at physiological pH where we can take advantage of the chemically modified carboxy-methyl $\text{cyt } c_{551}$ (as described below) whose stability at pH 3.0 would be too low for a quantitative characterization.

By reference to the canonical sequential pathway of cytochromes c folding (Scheme 1), the distal Fe–Met coordination bond is present only in the native state (N); its appearance in the $\text{cyt } c$ folding process can thus be used to monitor the formation of N . Therefore, we carried out an unfolding/refolding experiment following absorbance at 695 nm, which is diagnostic of the Fe–Met coordination bond in oxidized cytochromes c .³⁰ Since the transient intermediates I_c and M (depicted in Scheme 1) lack the native Fe–Met coordination bond, no refolding burst phase should be detected at this wavelength. However, inspection of the experiment in Figure 3, carried out at pH 3.0,

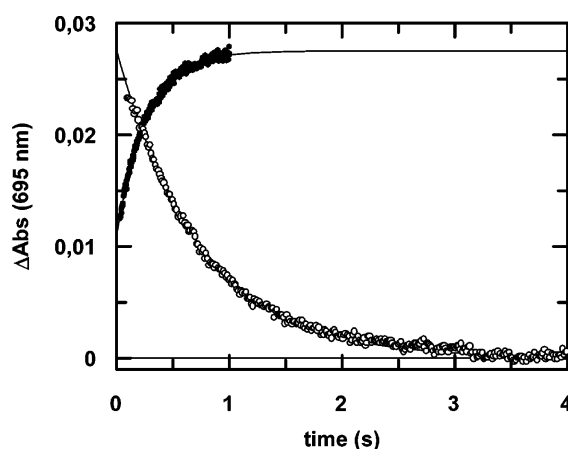


Figure 3. Unfolding (open circles) and refolding (filled circles) time course of oxidized $\text{cyt } c_{551}$ followed by absorbance at 695 nm. Results at pH 3.0 in the presence of 3.5 M GdnHCl for unfolding, and at 0.5 M GdnHCl for refolding; [$\text{cyt } c_{551}$] 50 μM after mixing. Continuous lines represent the best fit to a single exponential process.

shows that the refolding amplitude at 695 nm is much smaller than that observed in unfolding, being $\sim 50\%$ of the total change in signal. A direct comparison between unfolding and refolding amplitudes under these conditions is justified because the total amplitude of the 695 nm band seen in unfolding experiments is independent of urea concentration (data not shown).

The observation of a burst phase when refolding is monitored at 695 nm prompted us to probe more directly the role of this coordination bond in the folding mechanism. Therefore we prepared a chemically modified cyt c_{551} (carboxy-methyl cyt c_{551} , Cm-cyt c_{551}), which lacks the sixth coordination position because of the covalent modification of the distal Met residue.³¹ Spectroscopic and electron transfer studies on horse Cm-cyt c complexed with its redox partner, cytochrome c oxidase, have demonstrated that the protein maintains, by-and-large, its native three-dimensional structure.³² Cm-cyt c_{551} is therefore an appropriate model system for folding experiments, aimed at clarifying the kinetic and thermodynamic role of the Fe–Met coordination bond. Fluorescence quenching was employed to follow the refolding/unfolding kinetics of Cm-cyt c_{551} : at all urea concentrations, a

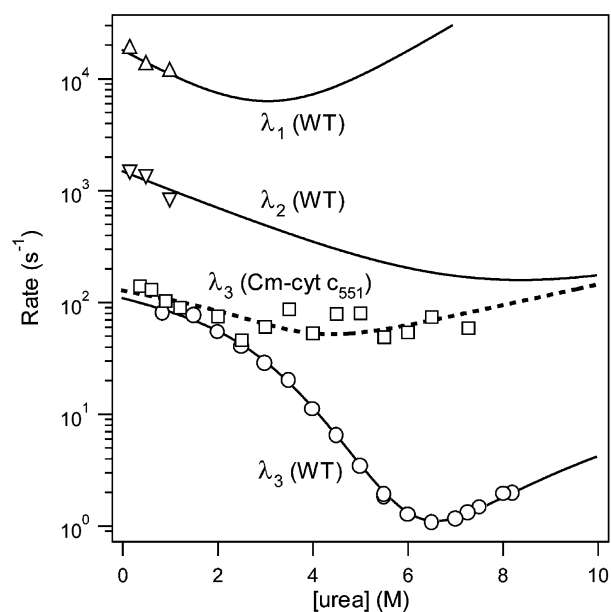


Figure 4. Urea-dependence of the rate constants for the rate-limiting folding/unfolding phase of wt cyt c_{551} (circles) and Cm-cyt c_{551} (squares) measured by stopped-flow fluorescence at pH 7.0 and 10 °C. Also shown are the rates of two additional phases on the sub-millisecond time scale observed by continuous-flow measurements on wt cyt c_{551} (triangles). The continuous lines show the observable rate constants predicted for unmodified cyt c_{551} , using Scheme 1. To simulate the main folding phase for Cm-cyt c_{551} (broken line), the same set of elementary rate constants was used, except that the rate constant for conversion of states N to M in Scheme 1 was increased by a factor 10^6 . This destabilizes state N and reduces Scheme 1 to a three-state mechanism, $U \rightleftharpoons I \rightleftharpoons M$, where M corresponds to the folded state of Cm-cyt c_{551} .

single exponential decay was observed, as with wt cyt c_{551} . A semilogarithmic plot of the observed unfolding/refolding rate constant as a function of [urea] (Chevron plot) for wt cyt c_{551} and Cm-cyt c_{551} at pH 7.0 is shown in Figure 4. Also included are the rates of two additional fast phases observed in continuous-flow fluorescence measurements on the unmodified protein at pH 7. Consistently with Scheme 1, in spite of the considerable destabilization of the folded state of Cm-cyt c_{551} compared to the wt protein ($\Delta\Delta G^0 \sim 5 \text{ kcal mol}^{-1}$), the observed refolding rates below 3 M urea are very similar for these two proteins, indicating that the Fe–Met coordination bond is formed after the transition state. This was confirmed by modeling the urea-dependent kinetics, based on Scheme 1. The continuous lines in Figure 4 represent the observable rate constants predicted by Scheme 1, using numeric simulations as described above. We first modeled the kinetics of the unmodified protein, using the data at pH 4.7 as a guideline. To simulate the folding kinetics of Cm-cyt c_{551} , it is sufficient to increase the rate of unfolding of N (k_{NM}) by several orders of magnitude, which renders N highly unstable. The folding reaction thus ends at the native-like intermediate M, which lacks the native methionine ligand and corresponds to the carboxy-methylated form. The agreement between the predicted and observed rates in both forms of the protein provides strong support for Scheme 1 as the basic folding model at physiological pH. Detailed insights on the role of the high energy intermediate M in the folding of cyt c_2 from *R. capsulatus* and cyt c_{551} from *P. aeruginosa* can be found in Sauder *et al.*²¹ and Gianni *et al.*²² respectively.

Discussion

The kinetic folding mechanism depicted in Scheme 1 and originally proposed for horse cyt c suggests that the Fe–Met coordination bond is present only in the native state (N). Kinetic characterization of the chemically modified carboxy-methylated cyt c_{551} (Cm-cyt c_{551}) is in agreement with this mechanism, indicating that the Met61–Fe coordination bond is formed only in the last stages of folding. It should be noted that the chemical modification of Met(61) introduces a considerable destabilization of the native state, as revealed by the large increase in the unfolding rate of Cm-cyt c_{551} ($k_{unf} \sim 40 \text{ s}^{-1}$ compared to $k_{unf} \sim 0.01 \text{ s}^{-1}$ for the unmodified protein).

In spite of these observations on the refolding behavior of Cm-cyt c_{551} and in contrast with Scheme 1, we find that a pronounced refolding burst phase ($\sim 50\%$) is detectable at pH 3 when the folding process of cyt c_{551} is followed by absorbance at 695 nm, monitoring the formation of the Met–Fe coordination bond (Figure 3). This finding indicates that $\sim 50\%$ of the native Fe–Met

coordination bond is formed during the stopped-flow dead-time (~ 2 ms).

Key findings to shed light on these two apparently contradictory observations are (i) the ultra-rapid continuous-flow mixing results at pH 4.7 (Figure 2), which show bi-exponential kinetics on the sub-millisecond time scale, and (ii) the double mixing interrupted refolding experiments at pH 3 (Figure 1) showing that the amplitude behavior of the observed single exponential unfolding decay implies that a fraction of wt cyt c_{551} refolds to the native state very rapidly (10 ms).

Some general models have been discussed to explain the kinetic partitioning between fast and slow refolding channels.^{28,33} A first model postulates the presence of a mixture of different unfolded states,³⁴ in this case, as long as refolding is rapid compared to the interconversion between these states, folding will occur *via* parallel pathways. Possible origins for multiplicity of unfolded states may be *cis-trans* equilibria of prolyl³⁵ and non-prolyl³⁶ peptide bonds. Another potential source of heterogeneity, in the case of heme proteins, is the presence of alternative axial heme ligands. In fact, interconversion between different unfolded states that leads to parallel folding pathways has also been identified for reduced horse cyt *c* in which, after CO photodissociation, the unfolded ensemble is represented by a distribution of different coordination states.³⁷ Alternatively, a possible scenario may predict parallel pathways even if folding starts from a homogenous unfolded state. This second model suggests that dilution of the denaturant may give rise to formation of kinetically trapped intermediates that fold more slowly, while the remainder of the unfolded molecules can fold rapidly resulting in the observed kinetic partitioning. Following this view, we recall that kinetic traps during refolding may originate from the formation of non-native inter-molecular interactions that give rise to transient aggregation,²⁵ as discussed also in the case of cyt c_{551} .²²

In the case of cyt c_{551} , (i) in addition to Met61, which ligates the iron in the native state, the other Met residue at position 22 cannot bind to the metal in the distal position, being too close in sequence to the heme attachment region (Cys12-Cys15/His16); and (ii) there are no histidine residues other than the native His16 ligand. Therefore non-native Met- or His-Fe interactions cannot occur. Nevertheless, although our analysis of Cm-Cyt c_{551} indicates that Met61 ligation is not involved in the rate-determining step in folding at low denaturant concentrations (Figure 4), we cannot rule out the possibility that heme ligation plays a role during the early stages of folding. The presence of a pronounced burst phase seen in refolding experiments has been previously attributed to the rapid accumulation of a collapsed state,²³ consistent with the direct observation of sub-millisecond processes in horse cyt *c*.¹² The kinetic heterogeneity observed in fast mixing experiments (Figure 2) indicates that the early

stages of folding of cyt c_{551} are complex and possibly imply more than the simple accumulation of an obligatory intermediate species. Even more compelling is the outcome of the refolding kinetics at 695 nm (Figure 3) and of the double mixing experiments shown in Figure 1. Thus a tentative description of the refolding pathway of cyt c_{551} may demand a mechanism with two (or more) parallel folding channels, such as Scheme 2 above.

Scheme 2 implies that the denatured state of cyt c_{551} consists of two (or more) distinct populations of states, U and U', undergoing slow inter-conversion (>1 second). The relative populations of U and U' vary strongly with pH. At pH 4.7, U' accounts for about 20% of the population and grows to about 50% at pH 3. If the net folding rate along the main folding pathway (U \rightarrow I_c \rightarrow M) remains similar at low pH, it might account for the rapidly accumulated (10 ms) folding species in the double-jump experiment (Figure 1). The pH-dependent partitioning between different denatured-state populations is consistent with previous observations²² that the equilibrium *m*-values for urea-induced unfolding are significantly higher at pH 3.0 (2.2 kcal mol⁻¹ M⁻¹) compared to pH 7.0 (1.1 kcal mol⁻¹ M⁻¹), suggesting that neutral pH conditions favor a more structured denatured state. Although a direct involvement of kinetic traps due to mis-ligation of the heme iron is unlikely, the increasing population of U' and concomitant decrease in the rate of folding at low pH may be related to protonation of the proximal histidine, His16, which is expected to occur under sufficiently acidic conditions. The resulting four-coordinate species would be highly reactive and may favor denatured-state populations containing non-native intra- or inter-molecular heme ligands.

Finally, in the more general context of comparative folding studies on the family of class I cytochromes *c*, we have presented evidence that the burst phase observed by stopped-flow fluorescence underlies a more complex picture (Scheme 2) than previously assumed, which may not be explained solely by the sequential accumulation of partially structured intermediates. From this perspective, the description of the early events of *in vitro* cyt *c* folding may have to be re-assessed, taking into account the relative fluorescence of the native state, the collapsed intermediate and eventually aggregated forms. It is possible that this protein family presents a variety of folding mechanisms that may, or may not, involve accumulation of intermediate states, depending on the specific sequence propensities to form elements of secondary structure.^{7,22,38}

Materials and Methods

Materials

Recombinant cyt c_{551} from *P. aeruginosa* was expressed and purified as described.³⁹ All experiments were carried

out on the oxidized protein, as checked spectrophotometrically.

Cm-cyt c_{551} was prepared and purified as described.³¹ The fraction of Cm-cyt c_{551} after purification was more than 95%, as judged by CO titration of reduced Cm-cyt c_{551} at pH 7.0 (data not shown). All reagents were of analytical grade.

Stopped-flow measurements

All fluorescence-detected kinetic folding experiments were carried out on an Applied Photophysics DX-17MV stopped-flow instrument (Leatherhead, UK); the excitation wavelength was 290 nm and the fluorescence emission was measured using a 320 nm cut-off glass filter. In all experiments, performed at 10 °C, refolding and unfolding were initiated by an 11-fold dilution of the denatured or the native protein in the appropriate buffer.

Double-jump mixing measurements

Interrupted refolding experiments were carried out on an Applied Photophysics DX-17MV stopped-flow instrument with double jump facility (Leatherhead, UK) in order to assess the time dependence of accumulation of the native state, which unfolds slowly after the second mixing. The excitation wavelength was 290 nm and the fluorescence emission was measured using a 320 nm cut-off glass filter. Refolding and unfolding were initiated by a symmetric mixing of the denatured and native protein with the appropriate buffer. Unfolded cyt c_{551} was obtained by incubation in 0.8 M GdnHCl at pH 2.0, the protein being totally unfolded as judged by far UV CD spectroscopy (data not shown). When an additional control was carried out by mixing equal volumes of unfolded cyt c_{551} in 0.4 M GdnHCl at pH 2 with 4 M GdnHCl at pH 3.0, no relevant change in signal was observed (data not shown).

Continuous flow measurements

Continuous flow measurements were performed using the instrument described by Shastry *et al.*²⁷ Total flow rate was 0.8 ml s⁻¹. The instrumental dead time, calibrated by measuring the quenching of *N*-acetyltryptophanamide fluorescence by *N*-bromo succinimide at several quencher concentrations, was 60 μs in the absence of denaturant. Temperature (15 °C) was regulated by cooling the chamber surrounding both the cuvette and the flow lines.

Acknowledgements

Work partially supported by grants from the Ministero dell' Istruzione, Università e Ricerca and Consiglio Nazionale delle Ricerche of Italy (PRIN 2001 on "Structural dynamics of heme-proteins" and Progetto Strategico "Genetica Molecolare" CTB-CNR 01.00856.ST97), by grants MCB-079148 from the National Science Foundation of the USA and CA06927 from the NIH (to H. R.) and an appropriation from the Commonwealth of Pennsylvania to the Fox Chase Cancer Center. We

thank Mr Dagai and Dr Nicolini (Istituto Superiore di Sanità, Rome) for their assistance with large-scale bacterial growth.

References

1. Matouschek, A., Kellis, J. T., Jr, Serrano, L., Bycroft, M. & Fersht, A. R. (1990). Transient folding intermediates characterized by protein engineering. *Nature*, **346**, 440–445.
2. Parker, M. J., Spencer, J. & Clarke, A. R. (1995). An integrated kinetic analysis of intermediates and transition states in protein folding reactions. *J. Mol. Biol.* **253**, 771–786.
3. Khorasanizadeh, S., Peters, I. D. & Roder, H. (1996). Evidence for a three-state model of protein folding from kinetic analysis of ubiquitin variants with altered core residues. *Nature Struct. Biol.* **3**, 193–205.
4. Wolynes, P. G., Onuchic, J. N. & Thirumalai, D. (1995). Navigating the folding routes. *Science*, **268**, 959–961.
5. Dill, K. A. & Chan, H. S. (1997). From Levinthal to pathways to funnels. *Nature Struct. Biol.* **10**, 19.
6. Lazaridis, T. & Karplus, M. (1997). "New view" of protein folding reconciled with the old through multiple unfolding simulations. *Science*, **278**, 1928–1931.
7. Colón, W., Elöve, G. A., Wakem, L. P., Sherman, F. & Roder, H. (1996). Side chain packing of the N- and C-terminal helices plays a critical role in the kinetics of cytochrome *c* folding. *Biochemistry*, **35**, 5538–5549.
8. Colón, W., Waken, L. P., Sherman, F. & Roder, H. (1997). Identification of the predominant non-native histidine ligand in unfolded cytochrome *c*. *Biochemistry*, **36**, 12535–12541.
9. Sosnick, T. R., Shtilerman, M. D., Mayne, L. & Englander, S. W. (1997). Ultrafast signals in protein folding and the polypeptide contracted state. *Proc. Natl Acad. Sci. USA*, **94**, 8545–8550.
10. Chan, C.-K., Hu, Y., Takahashi, S., Rousseau, D. L., Eaton, W. A. & Hofrichter, J. (1997). Submillisecond protein folding kinetics studied by ultrarapid mixing. *Proc. Natl Acad. Sci. USA*, **94**, 1779–1784.
11. Takahashi, S., Yeh, S. R., Das, T. K., Chan, C. K., Gottfried, D. S. & Rousseau, D. L. (1997). Folding of cytochrome *c* initiated by submillisecond mixing. *Nature Struct. Biol.* **1**, 44–50.
12. Shastry, R. M. C. & Roder, H. (1998). Evidence for barrier-limited protein folding kinetics on the microsecond time scale. *Nature Struct. Biol.* **5**, 385–392.
13. Pollack, L., Tate, M. W., Darnton, N. C., Knight, J. B., Gruner, S. M., Eaton, W. A. & Austin, R. H. (1999). Compactness of the denatured state of a fast-folding protein measured by submillisecond small-angle X-ray scattering. *Proc. Natl Acad. Sci. USA*, **96**, 10115–10117.
14. Akiyama, S., Takahashi, S., Ishimori, K. & Morishima, I. (2000). Stepwise formation of alpha-helices during cytochrome *c* folding. *Nature Struct. Biol.* **6**, 443–445.
15. Hagen, S. J. & Eaton, W. A. (2000). Two-state expansion and collapse of a polypeptide. *J. Mol. Biol.* **301**, 1019–1027.
16. Roder, H., Elöve, G. A. & Englander, S. W. (1988). Structural characterization of folding intermediates in cytochrome *c* by H-exchange labelling and proton NMR. *Nature*, **335**, 700–704.
17. Sauder, J. M. & Roder, H. (1998). Amide protection in

- an early intermediate of cytochrome *c*. *Fold. Des.* **4**, 293–301.
18. Yeh, S. R. & Rousseau, D. L. (1998). Folding intermediates in cytochrome *c*. *Nature Struct. Biol.* **5**, 222–228.
 19. Telford, J. R., Tezcan, F. A., Gray, H. B. & Winkler, J. R. (1999). Role of ligand substitution in ferrocycytochrome *c* folding. *Biochemistry*, **38**, 1944–1949.
 20. Rumbley, J., Hoang, L., Mayne, L. & Englander, S. W. (2001). An amino acid code for protein folding. *Proc. Natl Acad. Sci. USA*, **98**, 105–112.
 21. Sauder, J. M., MacKenzie, N. E. & Roder, H. (1996). Kinetic mechanism of folding and unfolding of *Rhodobacter capsulatus* cytochrome *c*₂. *Biochemistry*, **35**, 16852–16862.
 22. Gianni, S., Travaglini-Allocatelli, C., Cutruzzolà, F., Bigotti, M. G. & Brunori, M. (2001). Snapshots of protein folding A study on the multiple transition state pathway of cytochrome *c*₅₅₁ from *Pseudomonas aeruginosa*. *J. Mol. Biol.* **309**, 1177–1187.
 23. Travaglini-Allocatelli, C., Cutruzzolà, F., Bigotti, M. G., Staniforth, R. A. & Brunori, M. (1999). Folding mechanism of *Pseudomonas aeruginosa* cytochrome *c*₅₅₁: role of electrostatic interactions on the hydrophobic collapse and transition state properties. *J. Mol. Biol.* **289**, 1459–1467.
 24. McGee, W. A. & Nall, B. T. (1998). Refolding rate of stability-enhanced cytochrome *c* is independent of thermodynamic driving force. *Protein Sci.* **7**, 1071–1082.
 25. Silow, M. & Oliveberg, M. (1997). Transient aggregates in protein folding are easily mistaken for folding intermediates. *Proc. Natl Acad. Sci. USA*, **94**, 6084–6086.
 26. Oliveberg, M., Tan, Y. J., Silow, M. & Fersht, A. R. (1998). The changing nature of the protein folding transition state: implication for the shape of the free-energy profile for folding. *J. Mol. Biol.* **277**, 933–943.
 27. Shastry, R. M. C., Luck, S. D. & Roder, H. (1998). A continuous-flow capillary mixing method to monitor reactions on the microsecond time scale. *Biophys. J.* **74**, 2714–2721.
 28. Kiefhaber, T. (1995). Kinetic traps in lysozyme folding. *Proc. Natl Acad. Sci. USA*, **92**, 9029–9033.
 29. Jackson, S. E. & Fersht, A. R. (1991). Folding of chymotrypsin inhibitor 2. 1. Evidence for a two-state transition. *Biochemistry*, **30**, 10428–10435.
 30. Harbury, H. A., Cronin, J. R., Fanger, M. W., Hettinger, T. P., Murphy, A. J., Myer, Y. P. & Vinogradov, S. N. (1965). Complex formation between methionine and a heme peptide from cytochrome *c*. *Proc. Natl Acad. Sci. USA*, **54**, 1658–1664.
 31. Brunori, M., Wilson, M. T. & Antonini, E. (1972). Properties of modified cytochromes. I. Equilibrium and kinetics of the pH-dependent transition in carboxymethylated horse heart cytochrome *c*. *J. Biol. Chem.* **247**, 6076–6081.
 32. Brzezinski, P. & Wilson, M. T. (1997). Photochemical electron injection into redox-active proteins. *Proc. Natl Acad. Sci. USA*, **94**, 6176–6179.
 33. Wallace, L. A. & Matthews, C. R. (2002). Sequential versus parallel protein-folding mechanisms: experimental tests for complex folding reactions. *Biophys. Chem.* **101–102**, 113–131.
 34. Lee, J. C., Engman, K. C., Tezcan, A., Gray, H. B. & Winkler, J. R. (2002). Structural features of cytochrome *c*' folding intermediates revealed by fluorescence energy-transfer kinetics. *Proc. Natl Acad. Sci. USA*, **99**, 14778–14782.
 35. Kiefhaber, T., Kohler, H. H. & Schmid, F. X. (1992). Kinetic coupling between protein folding and prolyl isomerization. I. Theoretical models. *J. Mol. Biol.* **224**, 217–229.
 36. Pappenberger, G., Aygun, H., Engels, J. W., Reimer, U., Feisher, G. & Kiefhaber, T. (2001). Nonprolyl *cis* peptide bonds in unfolded proteins cause complex folding kinetics. *Nature Struct. Biol.* **8**, 452–458.
 37. Goldbeck, R. A., Thomas, Y. G., Chen, E., Esquerra, R. M. & Kliger, D. S. (1999). Multiple pathways on a protein folding energy landscape: kinetic evidence. *Proc. Natl Acad. Sci. USA*, **96**, 2782–2787.
 38. Guidry, J. & Wittung-Stafshede, P. (2000). cytochrome *c*₅₅₃, a small heme protein that lacks misligation in its unfolded state, folds with rapid two-state kinetics. *J. Mol. Biol.* **301**, 769–773.
 39. Cutruzzolà, F., Ciabatti, I., Rolli, G., Falcinelli, S., Arese, M., Ranghino, G. *et al.* (1997). Expression and characterization of *Pseudomonas aeruginosa* cytochrome *c*₅₅₁ and two site-directed mutants: role of tryptophan 56 in the modulation of redox properties. *Biochem. J.* **322**, 35–42.

Edited by C. R. Matthews

(Received 23 December 2002; received in revised form 20 May 2003; accepted 20 May 2003)